Harnessing advanced tractography in neurosurgical practice

Ahmad Beyh[1,3], Ann-Katrin Ohlerth[2] & Stephanie J. Forkel[3-5]

[1] *Department of Psychiatry, Brain Health Institute, Rutgers University, Piscataway, NJ, USA*

[2] *Neurobiology of Language Department, Max Planck Institute for Psycholinguistics, Nijmegen, the Netherlands*

[3] *Donders Institute for Brain Cognition Behaviour, Radboud University, Nijmegen, the Netherlands*

[4] *Brain Connectivity and Behaviour Laboratory, Sorbonne Universities, Paris, France*

[5] *Centre for Neuroimaging Sciences, Department of Neuroimaging, Institute of Psychiatry, Psychology and Neuroscience, King's College London, London, UK*

Authors' OrchIDs

AB 0000-0001-9071-0150, AKO 0000-0001-6662-9002, SJF 0000-0003-0493-0283

ABSTRACT

This chapter explores the fundamentals and recent advancements of diffusion-weighted imaging (DWI) and its primary application, tractography. Both have become indispensable in the research arena and are currently being integrated into the clinical world, especially for neurosurgery. These technologies provide rapid, *in vivo* mapping of white matter tracts, greatly assisting surgeons in pre-surgical planning and enabling them to offer patients more precise prognostic information, thereby enhancing the process of informed decision-making. Despite nearly three decades of use in research and the development of sophisticated mapping techniques, the adoption of contemporary tractography methods in clinical settings has been slow. Here, we aim to provide a comprehensive understanding of DWI's basic principles, shed light on advanced methodologies that surpass the traditional diffusion tensor model, and discuss the clinical integration of tractography. Our objective is to advocate for incorporating newer tractography techniques into standard clinical practice.

Keywords: Brain tumour, Diffusion tensor imaging, High Angular Resolution Diffusion Imaging, White matter, Tractography

Introduction

In the dynamic field of neurosurgery, the need for cutting-edge methods is increasingly critical. As neurosurgical approaches become more multimodal and technologically advanced, the central role of white matter tracts in the brain and the imperative of their precise preoperative mapping is gaining recognition. Advanced tractography is a vital tool for neurosurgeons, offering unparalleled *in vivo* delineation and visualisation of these complex neural pathways.

This chapter addresses the urgent need for advanced tractography in modern neurosurgery and discusses how its application can profoundly improve surgical planning, execution, and patients' cognitive and behavioural outcomes. Initially, we will examine the basic concepts of diffusion-weighted imaging (DWI), the foundational bedrock for advanced tractography techniques. Subsequently, we will venture beyond the limitations of traditional tractography, critically examining the shortcomings of diffusion tensor imaging (DTI), and advocating for the integration of more sophisticated imaging techniques in surgical practice. Books and reviews have been written on this topic (e.g., Jones, 2010; Le Bihan & Johansen-Berg, 2012), and we do not aim to cover the theory in depth, but we will offer a brief overview of the concepts that we believe are central to understanding the methods and their applications in the context of neurosurgery.

Part 1: Neuroimaging

From diffusion-weighted imaging to advanced tractography

Diffusion-weighted imaging (DWI)

Diffusion refers not to the large-scale movement of water molecules but to their small-scale, erratic movements akin to a 'random walk' pattern (see Figure 1). In the brain, water molecules within various tissue types engage in this diffusion process, randomly 'exploring' their immediate surroundings at a microscopic level. The speed of this diffusion process is influenced by several factors, including temperature and the

characteristics of the surrounding environment, and is quantified as the apparent diffusion coefficient (ADC; Le Bihan, 2013). This concept is fundamental to diffusion imaging, which utilises the variable nature of diffusion to investigate tissue microstructure and non-invasively chart white matter pathways (i.e., tractography).

DWI is typically acquired using a spin-echo echo planar imaging (SE-EPI) MRI pulse sequence (Basser atl al., 1994). This technique quickly applies and removes diffusion-weighting magnetic gradients, which affect the imaged protons. When a diffusion gradient is applied, protons diffusing parallel to its primary direction experience a reduction in signal. In contrast, those that are stationary or moving in other directions do not, or experience less attenuation. Consequently, DWI extracts information about water diffusion from the amount of signal reduction caused by each diffusion gradient (Figure 2). The characteristics of the applied diffusion gradients are encapsulated in a term called the 'b-value', measured in s/mm². Higher b-values diminish the signal from rapid diffusion, e.g., in cerebrospinal fluid (CSF) or in grey matter, and enhance the detection of slow or restricted water diffusion, e.g., in deep white matter. However, as this is contingent upon greater overall signal attenuation, it also lowers the signal-to-noise ratio (SNR). As increasing image resolution also reduces SNR, the use of high b-values can be a challenge for some 1.5T scanners.

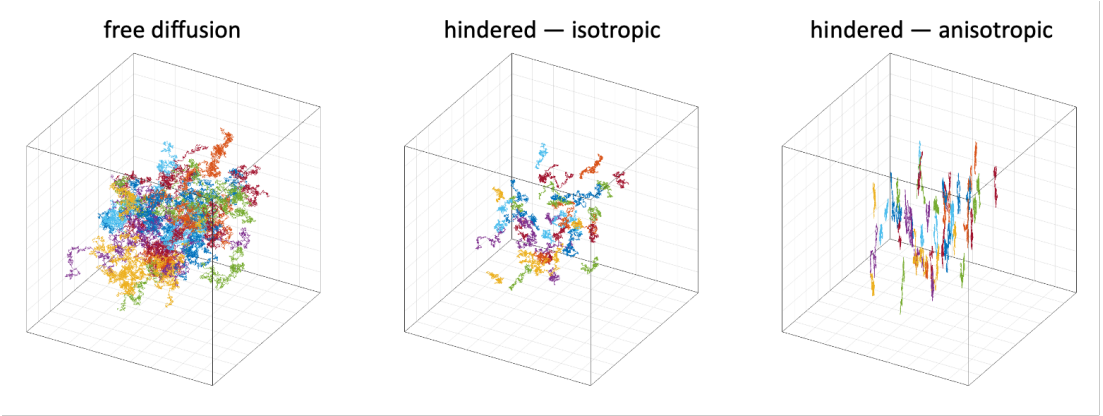

FIGURE 1. Patterns of water diffusion. In each panel, different colours represent the trajectories of different water molecules diffusing under certain conditions. Over time, a group of water molecules will move and randomly explore their surroundings in a jittery manner. In unrestricted or free diffusion, each molecule is free to move in all directions without any hindrance, resulting in an isotropic (i.e., equal in all directions) diffusion pattern. However, if these molecules are in an environment with other materials that restrict their movement, their diffusion pattern will be influenced by the arrangement of these materials. In a setting with isotropic hindrance, although each molecule can still move equally in all directions, the distance it can travel is limited due to obstructions from evenly dispersed barriers (hindered — isotropic). In an environment with uneven hindrance, the diffusion of water molecules is influenced by a spatial arrangement that

creates more obstacles in specific directions than others, resulting in distinct anisotropic diffusion patterns (hindered — anisotropic).

The observed signal attenuation due to protons diffusing along the diffusion gradient direction can be formalised according to the simplified Stejskal-Tanner equation (Stejskal & Tanner, 1965):

$$S = S_0 \cdot e^{-b \cdot ADC} \quad \text{(eq. 1)}$$

where S is the measured diffusion-weighted signal, S_0 is the signal acquired without diffusion weighting (equivalent to a T2-weighted signal) and typically referred to as the b0 image; b is the b-value; and ADC is the variable whose value will change depending on the tissue being imaged. ADC values are highest in CSF, followed by grey matter, then white matter (Le Bihan, 2013), and can be calculated directly from the measured DWI data without resorting to complex models:

$$ADC = \frac{-ln\left(\frac{S}{S_0}\right)}{b} \quad \text{(eq. 2)}$$

where ln is the natural logarithm. In this context, S and S_0 are the measured reference signal (b0 image) and diffusion-weighted signal (diffusion series), respectively.

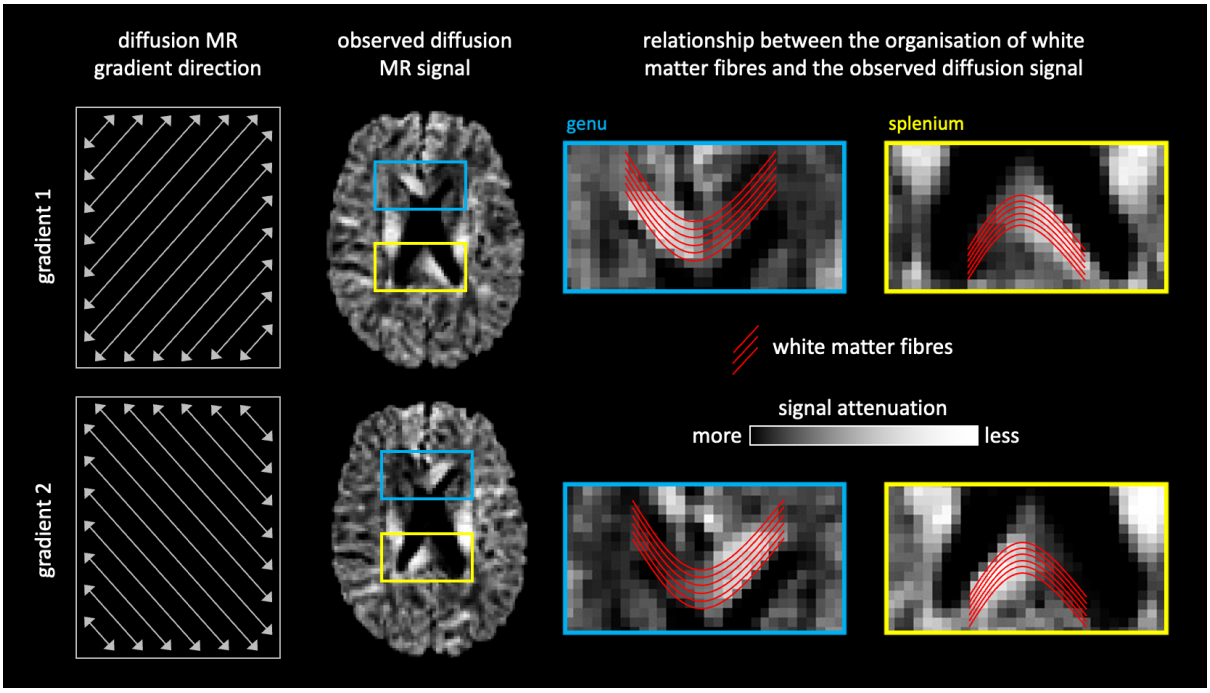

FIGURE 2. Diffusion-weighted imaging. In DWI, the MRI sequence includes diffusion-weighting gradients that cause a signal attenuation if the imaged tissue contains water molecules that diffuse along the gradient's direction. However, if the primary axis of water diffusion is perpendicular to

the gradient's direction, no attenuation is observed. This is what allows us to derive a measure of angular contrast within each voxel. Notice, e.g., that the genu and splenium of the corpus callosum look drastically different under the influence of each gradient.

The Tensor Model

Basser, Mattiello, and Le Bihan (1994) proposed the diffusion tensor model as a simultaneous representation of the ADC and the direction of water diffusion. The rationale is that probing water diffusion along six or more non-collinear directions yields enough information to mathematically model the displacement of the water molecules. The diffusion tensor is thus a three-dimensional ellipsoid with three principal axes, each characterised by a vector of a specific orientation (eigenvector), whose length (eigenvalue) is equivalent to the ADC along that axis. Several metrics are usually derived from the tensor in each voxel, the most common being fractional anisotropy (FA) and mean diffusivity (MD; Forkel & Catani, 2017). FA characterises the shape of the tensor, with high values in the white matter and near-zero values in CSF, while MD has the highest values in CSF and the smallest in the deep white matter where diffusion is most hindered.

Though widely successful, the tensor model has inherent limitations that impede the interpretation of derived microstructural measures and the accuracy of resultant tractography reconstructions (Figure 3). Diffusion Tensor Imaging (DTI) tractography assumes that water diffusion in any voxel is accurately represented by a single direction, as indicated by the tensor's principal eigenvector. However, this assumption is often violated — it is estimated that 60% to 90% of white matter voxels contain multiple fibre populations travelling along different orientations (Dell'Acqua et al., 2013; Tournier et al., 2011). As a result, the diffusion tensor would appear spherical in a voxel where three fibre populations intersect at right angles. This representation obscures the true orientations of the individual fibre populations and yields a low FA value. This not only leads to an inaccurate representation of the direction of water diffusion within the voxel, but could also cause the premature termination of tractography tracking due to the resultant low FA, as DTI-based algorithms are constrained by an FA threshold usually close to 0.15 during tracking (see Figure 3 for examples of these limitations).

Despite its limitations, DTI continues to be favoured for its simplicity and its relatively low demands on acquisition and computational resources. This is particularly the case in clinical settings, where the practical requirements often precede the use of more sophisticated acquisition techniques and complex modelling.

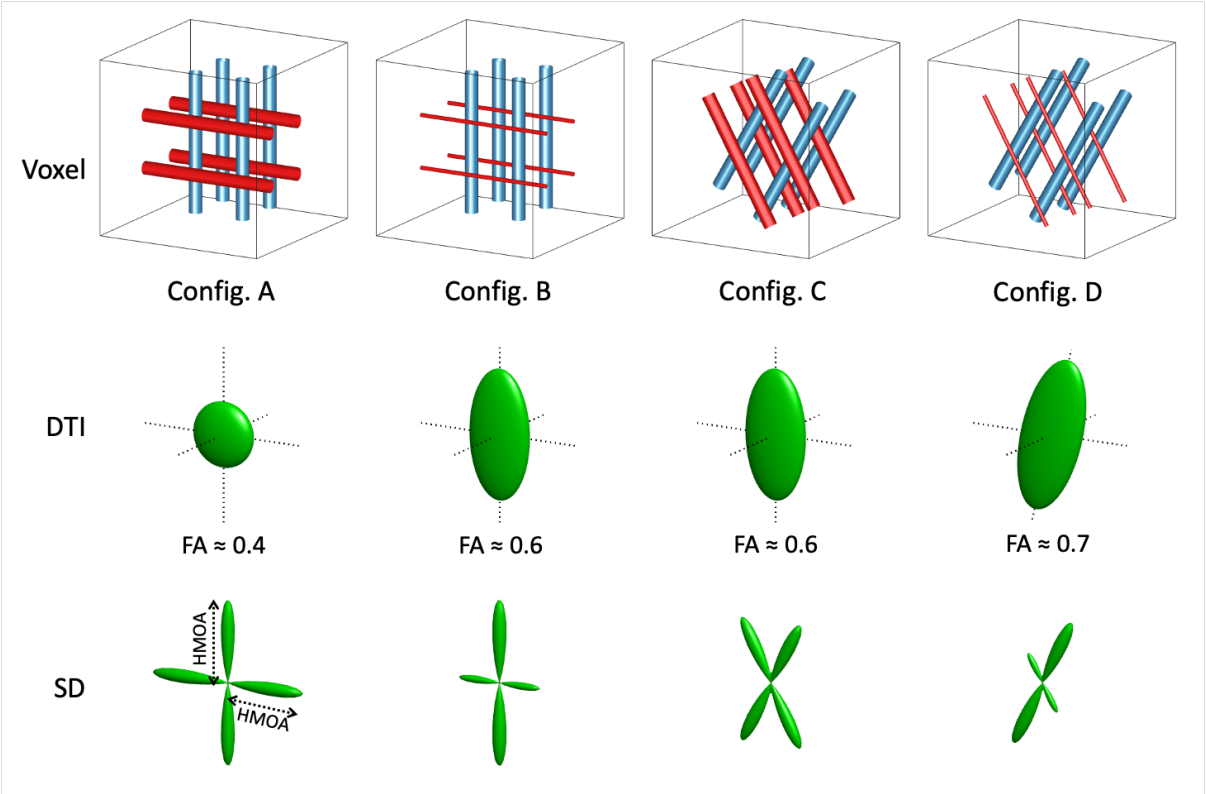

FIGURE 3. Multifibre anatomy and their construction using DTI and SD. The tensor model has a notable shortcoming in its inability to distinguish crossing fibres. For example, in configuration A, two fibre populations intersecting at right angles are represented as a flat tensor with a low fractional anisotropy (FA) value and with no correct principal axis, leading to erroneous tracking or might stop the process altogether. Moreover, identical tensors can result from two distinct fibre configurations, as seen in configurations B and C. In configuration D, the deterioration of one set of crossing fibres alters the tensor's shape, FA, and orientation, leading to a different tractography result. While DTI fails to differentiate these scenarios, spherical deconvolution (SD) can. This technique is capable of distinguishing between intersecting fibre populations within voxels and detecting fibre-specific changes, such as the degeneration of one fibre group in configuration D. This is achieved using the hindrance modulated orientational anisotropy (HMOA) metric, which provides an indication of fibre density.

Spherical Deconvolution (SD)

High angular resolution diffusion imaging (HARDI) refers to a family of advanced imaging tools developed by various research groups to address the main limitations of the tensor model. Although many HARDI methods have been proposed over time, such as Q-ball imaging (Tuch, 2004) and diffusion spectrum imaging (DSI; Wedeen et al., 2005), we focus

here on spherical deconvolution (SD; Dell'Acqua et al., 2010, 2013, Tournier, 2007), which has been optimised with anatomical models, and whose technical requirements are close to those of DTI.

SD operates under the premise that the diffusion signal measured in a voxel that contains multiple fibre populations is the sum of the fibre-specific signals within that voxel. SD conceptualises these populations as a continuous distribution of fibre orientations. In this framework, the signal is modelled as a spherical convolution (akin to a 'shape multiplication') between the fibre orientation density function (fODF) and a fibre response function. Therefore, when a diffusion signal is measured along multiple directions using MRI, it can be deconvolved using that fibre response function to estimate fibre orientations. The spherical deconvolution process yields the fibre orientation distribution (FOD). This multi-peak spherical function represents the orientations of the fibre populations traversing a voxel and their respective contributions to the signal (Figure 4).

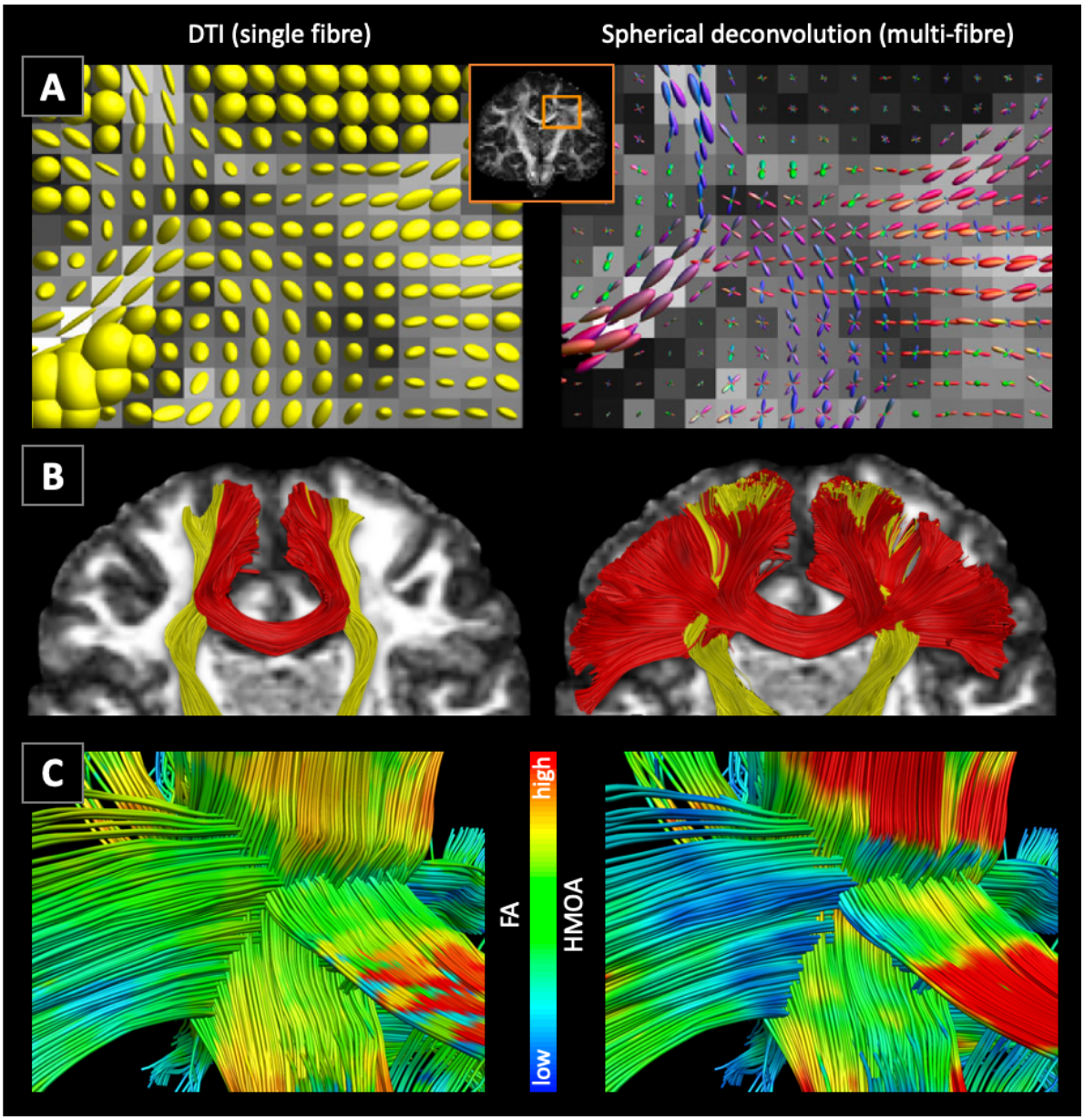

FIGURE 4. Single fibre vs. multi-fibre tractography. The tensor model (left) can only represent one fibre direction in each voxel, while spherical deconvolution (SD, right) can represent multiple fibre orientations as a fibre orientation distribution function (fODF). These butterfly-shaped 3D functions are then used by tracking algorithms to explore multiple white matter trajectories that can cross the same physical location in the brain. The region highlighted in panel A is the centrum semiovale, which houses at least three orthogonally crossing white matter pathways: the corticospinal tract, the corpus callosum, and the superior longitudinal fasciculus. All three fibre populations are captured by the fODFs in this region. Panel B clearly demonstrates DTI's inability to capture such complex information, with the classical limited reconstruction of the corpus callosum that only connects the medial cortical areas. In contrast, SD captures the full fanning of the callosal fibres. Panel C depicts the microstructural specificity of the multi-fibre approaches, which can attribute a different microstructural measure to each of the fibre populations crossing the same voxel. The image in panel A is adapted from Dell'Acqua & Tournier (2019) with permission (CC-BY); the images in panel B and C are inspired by Dell'Acqua & Catani (2012).

The FOD yields valuable insights into microstructure due to its capacity to represent multiple fibre orientations. A key measure the FOD provides is the number of fibre orientations (NuFO) within each voxel (Dell'Acqua et al., 2013), which is particularly useful in studies tracking degeneration over time. Another significant measure derived from the FOD is the hindrance-modulated orientational anisotropy (HMOA; Dell'Acqua et al., 2013), which is specific to each lobe of the FOD and relates to its magnitude, representing the apparent density of the represented fibre population. Lastly, the FOD facilitates multi-fibre tractography, which is a significant advancement over the conventional single-fibre tensor model.

SD necessitates the acquisition of diffusion data at elevated b-values to achieve high angular resolution and resolve intersecting fibres. While higher b-values enhance angular contrast, they also reduce SNR, so values in the range of 2000–3000 s/mm² are a good middleground and considered optimal for most tractography studies (Dell'Acqua and Tournier, 2019). Additionally, SD demands measuring the diffusion signal across numerous non-collinear diffusion directions. In contrast to DTI, which can be theoretically modelled with as few as six directions (though this is far from recommended), SD typically requires at least 45 directions to yield meaningful results, with 60 being the recommended number for most studies. While most current research studies gather data suitable for SD, this practice has not yet become standard in clinical settings.

SD tractography

SD tractography operates on principles similar to DTI tractography but uses directional information obtained from the FOD instead of the diffusion tensor. When streamline propagation begins, several checks are performed at each step to ensure accurate reconstruction of fibre paths. A notable difference is that in areas where the FOD shows multiple distinct peaks, an equivalent number of streamlines are initiated, matching the number of peaks. A critical distinction between SD and DTI tractography lies in the criteria that halt streamline propagation. An FA threshold, angular threshold, and step size guide tensor tractography; SD tractography uses HMOA as one of its four stopping criteria. Thus, the four guiding parameters for SD tractography include streamline length, step size, the maximum angle threshold, and the minimum HMOA value.

The technique outlined above is known as deterministic tracking, where a single streamline originates from each lobe of the FOD in every voxel. However, probabilistic tracking methods also offer certain benefits (as noted by Behrens et al., 2007; Descoteaux et al., 2009). In these methods, multiple streamlines are initiated from each FOD lobe, each following slightly varied paths. One method to establish these paths involves using the shape of the FOD to indicate the dispersion in the underlying fibre populations (Descoteaux et al., 2009). Narrower FOD lobes, resembling sticks, suggest the dominance of a single fibre population in the signal, while broader lobes imply the potential merging of multiple populations at close angles (<35 degrees). These populations may not be distinctly resolvable without using very high b-values, but their presence broadens the overall shape of the FOD lobe. In such cases, instead of only following the main FOD peak, which would lie between the two real ones, dispersion SD allows the tractography algorithm to take advantage of the information about anatomical uncertainty, thereby following the real directions. This approach effectively follows the true fibre directions and can be particularly advantageous for tracing smaller fibre bundles or those with highly curved trajectories.

Two of the most striking examples of the advantages of using SD tractography over standard DTI are its ability to visualise the lateral projections of the corpus callosum and the first and second branches of the superior longitudinal fasciculus (SLF; Thiebaut de Schotten et al., 2011) — all of which are impossible to reconstruct with the standard DTI tractography methods (Figure 4).

Advantages of using SD tractography

An alternative perspective on the distinction between DTI and SD techniques is that SD prioritises anatomical sensitivity, though this may lead to a higher rate of false positives especially if probabilistic tracking is used. In the context of pre-surgical planning, this enhanced sensitivity can be more beneficial for guiding surgical decisions. For example, when surgeons use tractography to determine the extent of tumour removal, SD tractography provides more detailed information about the underlying white matter anatomy, including how fibre bundles spread as they approach grey matter. This detailed mapping can guide a surgeon to opt for less aggressive resection near crucial white matter areas, especially if the patient prioritises functional preservation. This approach

also influences the use of distance metrics between a tumour and relevant white matter to predict surgical outcomes (Figure 5). It is crucial to emphasise that the gain in sensitivity offered by advanced methods also results in fibre bundles with larger volume (they occupy more white matter space), which will likely lead to a reduction of this distance. This nuanced understanding is pivotal for improving the accuracy of predictive models and, consequently, enhancing the reliability of distance-based assessments in neurosurgical planning.

Advanced multi-fibre tractography methods not only offer increased sensitivity but also yield more precise microstructural metrics (Figure 4). This precision arises from the ability of these methods to recognise multiple fibre orientations within a single voxel, each with distinct microstructural characteristics. A significant advantage of this approach is that the metrics are specific to individual fibres rather than to the voxel as a whole, making them highly suitable for tract-based analyses. For instance, in a study of a patient cohort with tumours near the corticospinal tract (CST), DTI-derived metrics like the voxel-based FA failed to reveal any microstructural differences between the ipsilateral and contralateral CST, but the tract-specific HMOA successfully identified these disparities (Mirchandani et al., 2021).

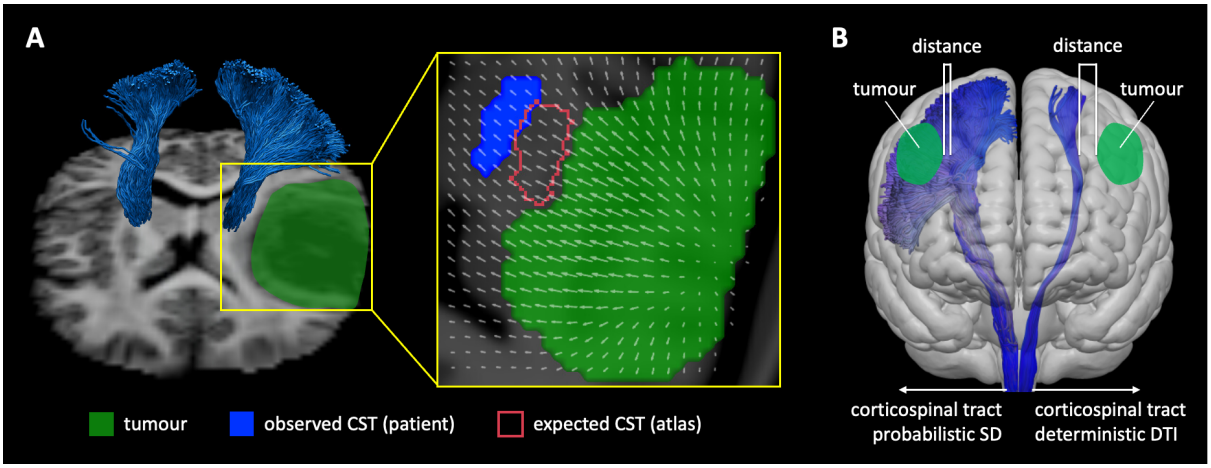

FIGURE 5. Technical considerations involved in tractography reconstructions for brain tumours. Panel (A) emphasises the limitations of atlas-based approaches due to white matter displacement. In this example, the tumour's expansion caused surrounding structures, including the corticospinal tract (CST), to shift medially, moving them away from their expected atlas-based location. Individualised tractography can accurately visualise these displaced connections, aiding in pre-surgical planning. The white arrows in the cutout panel represent the displacement field caused by the tumour's expansion. Panel (B) underscores the impact of algorithm selection on reconstruction reliability. The left-hand side image represents a probabilistic HARDI reconstruction, while the right-hand side panel shows a deterministic reconstruction. The core portion of the CST is visible in both, but the size of that core part is more prominent in the

probabilistic version, which also shows the entire cortical extent of the CST's projections. Image modified with permissions from the authors from (chapter ref to FLavio's handbook/ the preprint we put online).

Limitations of advanced tractography — or when to use classical DTI

Advanced tractography techniques have emerged as powerful tools for unravelling the intricacies of white matter fibre pathways within the brain, especially in fibre-dense areas. However, with this promise come limitations that necessitate careful consideration. The computational demands of some advanced tractography models can hinder their widespread use, particularly in clinical settings where quick results are essential. Additionally, these models depend heavily on high-quality diffusion MRI data; in situations where the data quality is subpar, the fidelity of the reconstruction can be disproportionately impacted, given the more exacting requirements of these techniques. Validating the results of advanced tractography proves challenging due to the complexity and user dependence of the algorithms involved (Schilling et al., 2019; Yendiki et al., 2022). This challenge raises questions about the clinical interpretability of advanced methods and has potentially hindered their uptake in the clinical world.

In contrast, DTI, though less intricate, remains widely used in the field, even in research studies. The standardisation and widespread availability of DTI make it a pragmatic choice in multicenter studies or clinical trials. Additionally, DTI algorithms have been refined to align with the white matter anatomy as revealed by postmortem dissections, thereby increasing the likelihood of accurately representing the white matter's central structures. Ultimately, the choice between advanced tractography and classical DTI hinges upon the unique demands of each study or clinical application, ranging from the necessity of rapid results and technical feasibility to the importance of standardised protocols and interpretability in varied clinical or research contexts.

Acquiring clinically suitable DWI data

To effectively utilise HARDI methods like spherical deconvolution, we will outline the essential components for conducting a successful DWI study using a clinical scanner. While additional recommendations could be made for more comprehensive research

studies where time is less constrained, we focus on identifying the fundamental elements that can deliver high-quality data within the tight time frames typical of a busy clinical setting. Consequently, the acquisition protocol we propose is designed to be feasible on most modern clinical scanners within a time frame of 5–7 minutes.

1. Use a b-value of 1500 s/mm^2 or higher to allow the chosen diffusion model to reliably separate fibres that cross the same voxel at angles as small as 40 degrees. Although higher b-values would be more desirable (e.g. 2000 s/mm^2), they may be challenging for clinical systems, so we recommend the more moderate choice of 1500 s/mm^2 as most modern clinical scanners can acquire images at such b-values without sacrificing data quality.

2. Acquire a minimum of 60 diffusion gradient directions. This covers the minimum requirement for models like spherical deconvolution and allows some leeway for cases where some volumes (directions) are lost due to motion or other artefacts.

3. Incorporate multiple b0 images into the sequence, with about three captured at the beginning and then one following every 10–15 volumes. This approach is beneficial during pre-processing and model fitting for two key reasons: firstly, acquiring several b0 images at the start guarantees that at least one or two are of high quality, even if the participant moves a lot during the initial 20 seconds of the acquisition. Secondly, interspersing b0 images throughout the sequence provides reference images at various points in the series, enhancing the robustness of motion correction models and simplifying quality control.

4. Pair the main acquisition with additional b0 images acquired with reverse-polarity phase encoding to be used for distortion correction (see pre-processing section). These images should have all imaging parameters exactly matched to the main acquisition except for the phase encoding direction. In theory, only one such image is required, but in practice, it is highly recommended to acquire at least three to ensure data viability in case of severe patient motion.

5. Use isotropic voxels of a minimum size of 2×2×2 mm^3, which is the most common resolution used in research studies until today.

6. Do not allow the scanner to automatically upsample the data, i.e. ensure that the voxel size is not changed by the scanner after the signal is collected, as is commonly done for some clinical structural sequences (see pre-processing section).

7. If the study involves patients who are unable to keep still for more than a few minutes at a time and good data cannot be acquired using the full-length MRI sequence, one could consider splitting the sequence into two sets of 30 different directions. This should be done as a last resort and only if no viable data can be acquired in a single go as it complicates data pre-processing. This will not be necessary on most modern clinical systems, which will have imaging acceleration features like multiband (or simultaneous multislice) that reduce the total acquisition time to approximately four minutes. If sequence splitting is done, during data pre-processing, these exams can be combined again to obtain the full set of 60 directions, for example, as done in Forkel et al., (2014). In this case, it is crucial to acquire a separate set of reverse phase encoded b0 images for each of the two halves of the acquisition, because a large head rotation during the short break between the two sets can result in different anatomical distortions (see pre-processing section on susceptibility distortions).

Other recommendations can be made for more advanced acquisitions that would typically result in longer exams but could be useful in a research context. For example, acquiring the diffusion signal using multiple b-values instead of one allows for more advanced and complex modelling of the signal and of tissue microstructure (these types of acquisitions are known as multi-shell diffusion studies). Pushing the b-value even higher, beyond 3000 s/mm^2 can be quite useful for the reconstruction of very small fibre bundles that cross larger ones at small angles. This, of course, would benefit from a research 3T scanner, which would also help in acquiring higher resolution images without losing too much SNR. To avoid pulsatile effects caused by cardiac events, cardiac-gated data can be acquired, which is to say that the MRI sequence can be time-locked to the cardiac cycle to ensure that images are acquired only during R-R intervals. These types of modifications would usually elongate the total exam time and depend on the scanner's capabilities, so they would not apply to most hospital-based clinical studies, but they are worth considering for patient cohorts acquired at research centres.

Data quality and pre-processing

Multiple elements influence the quality of MRI data, encompassing characteristics of the patient (such as movement during the scan, variations in heart rate and brain pulsations, or breathing patterns), aspects of the MRI sequence itself (like eddy current distortions, thermal noise, and Gibbs ringing), and interactions between the patient's anatomy and the scanner's environment (for example, susceptibility distortions). This section will discuss some of the primary artefacts typically addressed in DWI studies.

Head motion artefacts

Motion artefacts are a common issue in all imaging studies, not only in DWI, but they have a particularly significant impact in DWI. A standard DWI session lasts several minutes, during which it is crucial for the patient to remain as motionless as possible to reduce motion artefacts. A typical 2D EPI DWI sequence on a contemporary 1.5T or 3T scanner can complete a full brain scan (for one diffusion gradient direction) in 3–8 seconds, thanks to various scanning enhancements like imaging acceleration. This process of acquiring a single volume is repeated with varying diffusion weighting gradient directions until the entire set of images (e.g. 60 DWI volumes plus six b0 volumes) is captured. During this period, head motion can occur at any time and can compromise data quality within an individual volume (intra-volume motion) as well as affect the consistency of head position throughout the scan (inter-volume motion). See Figure 6 for examples of these artefacts.

The fundamental step involves addressing inter-volume motion, which is when the brain's position changes within the field of view from one volume to another. This type of correction is relatively straightforward and is achieved through rigid body alignment, ensuring that each voxel in the image matrix consistently aligns with the same anatomical location across the entire series of images. However, it is important to note that each volume acquisition takes several seconds, and any movement during this period can lead to two types of artefacts. The first is signal dropout, which is caused by head motion that takes place while an imaging slice is being acquired, leading to a mismatch between the imaging parameters and the slice's new position. This results in the appearance of dark

bands (slices) in the 3D image that can significantly disrupt model fitting if not properly corrected or if this happens frequently. The second artefact, resulting from intra-volume motion, appears as a 'zig-zag' pattern in the 3D volume when viewed perpendicular to the slice axis (such as a sagittal view of an axial acquisition). This occurs when the patient moves partway through acquiring a volume and remains in that new position, causing a misalignment in all slices imaged after that movement.

Some pre-processing tools take a model-based approach to correct for within-volume motion that results in signal dropout by exploiting the redundancy of the diffusion information in the data to regenerate the lost signal (Andersson et al., 2016). Others discard the slices with lost signal during the diffusion modelling step (Chang et al., 2005). Whichever approach is taken, accounting for signal dropout during pre-processing or modelling is a basic requirement, as it can have detrimental consequences during model fitting. Recent efforts have also been made to correct intra-volume motion with excellent results, albeit at a large computational cost (Andersson et al., 2017).

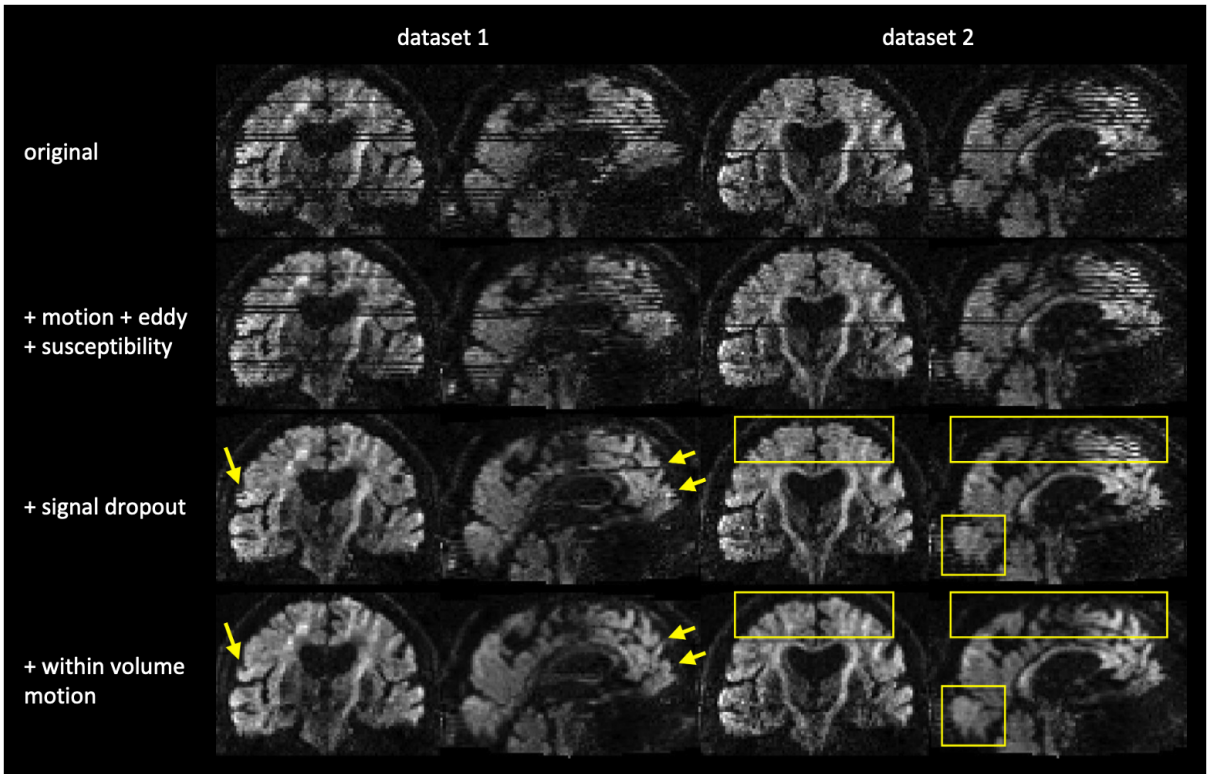

FIGURE 6. Motion correction of diffusion images. In addition to the framewise displacement caused by subject motion, other motion artefacts are observed in DWI data, including signal dropout and within volume misalignment. Here, two example datasets exhibit these artefacts. The top row represents the original data with all artefacts included; the second row represents data that have been corrected for framewise motion, eddy currents, and susceptibility distortions; the third row represents additional corrections for signal dropout; the last row represents a a full

correction that also accounts for within volume slice misalignment. Image adapted from Andersson et al. (2017) with permission (CC-BY).

Eddy current distortions

DWI pulse sequences involve the rapid introduction and removal of magnetic diffusion weighting gradients, a process that induces weak secondary magnetic fields due to interactions with the scanner's hardware and that interferes with the proton spins. This results in imaging artefacts known as eddy current distortions (Figure 7), which can compress, stretch, skew, or shift the imaged slice (Tournier et al., 2011). These distortions vary from one volume to the next as a function of the changing diffusion gradients and cause an anatomical mismatch between volumes, above and beyond the one caused by motion. Therefore, they must be properly dealt with during data pre-processing. Importantly, eddy currents are only present in the diffusion-weighted images but not in the b0 images that are acquired without any diffusion-weighting gradients. So, a commonly used approach to correcting these distortions is registering the diffusion-weighted volumes to the b0 image, which acts as an undistorted reference.

Susceptibility distortions

Different tissue types in and around the brain, such as grey and white matter, CSF, or air in the frontal sinuses, have different magnetic susceptibility properties. These tissue types are magnetised to different extents by the main magnetic field of the scanner, causing localised inhomogeneities in the effect of that magnetic field. This leads to localised and pronounced anatomical distortions that are common to EPI data, as in fMRI and DWI. The distortions cause a mismatch between the observed anatomy of the brain as imaged with EPI versus other MRI sequences that are robust to such effects, such as most structural T1-weighted or T2-weighted acquisitions. The most striking distortions occur in the orbitofrontal region due to the air-filled frontal sinuses and in the inferior temporal region due to the air-filled mastoid cells of the mastoid process. That being said, susceptibility distortions usually affect the entire brain.

Susceptibility distortions are restricted to the phase-encoding axis of the EPI sequence, which is the axis along which each slice of the image is read. We can exploit this feature

and acquire a few additional b0 images (i.e., without diffusion weighting) with the reverse phase encoding polarity, which will result in images with the same distortion magnitude but with the opposite distortion direction. The b0 images from the first acquisition and the reverse-phase b0 images can then be used to estimate the amount of distortion affecting each voxel and to correct the DWI data accordingly (Andersson & Sotiropoulos, 2016; Andersson et al., 2003). As susceptibility distortions depend on the interaction of the patient's anatomy with the scanner's main magnetic field, it follows that the distortions will change when the patient substantially rotates their head. It is therefore crucial to ensure that minimal movement takes place during the short time window separating the main diffusion acquisition from that of the reverse b0 images. More recent methods have been proposed to correct for these types of distortions by combining information from the b0 images and a T1w image, doing away with the need for the reverse phase data (Schilling et al., 2020). See an example of these distortions in Figure 7.

It is clear that this kind of correction is essential for DWI data, particularly when it is integrated with structural images for neurosurgical planning purposes. Regrettably, in many surgical departments, such corrections are often not implemented, primarily due to the absence of support for these corrective measures in the standard image processing software used in hospitals.

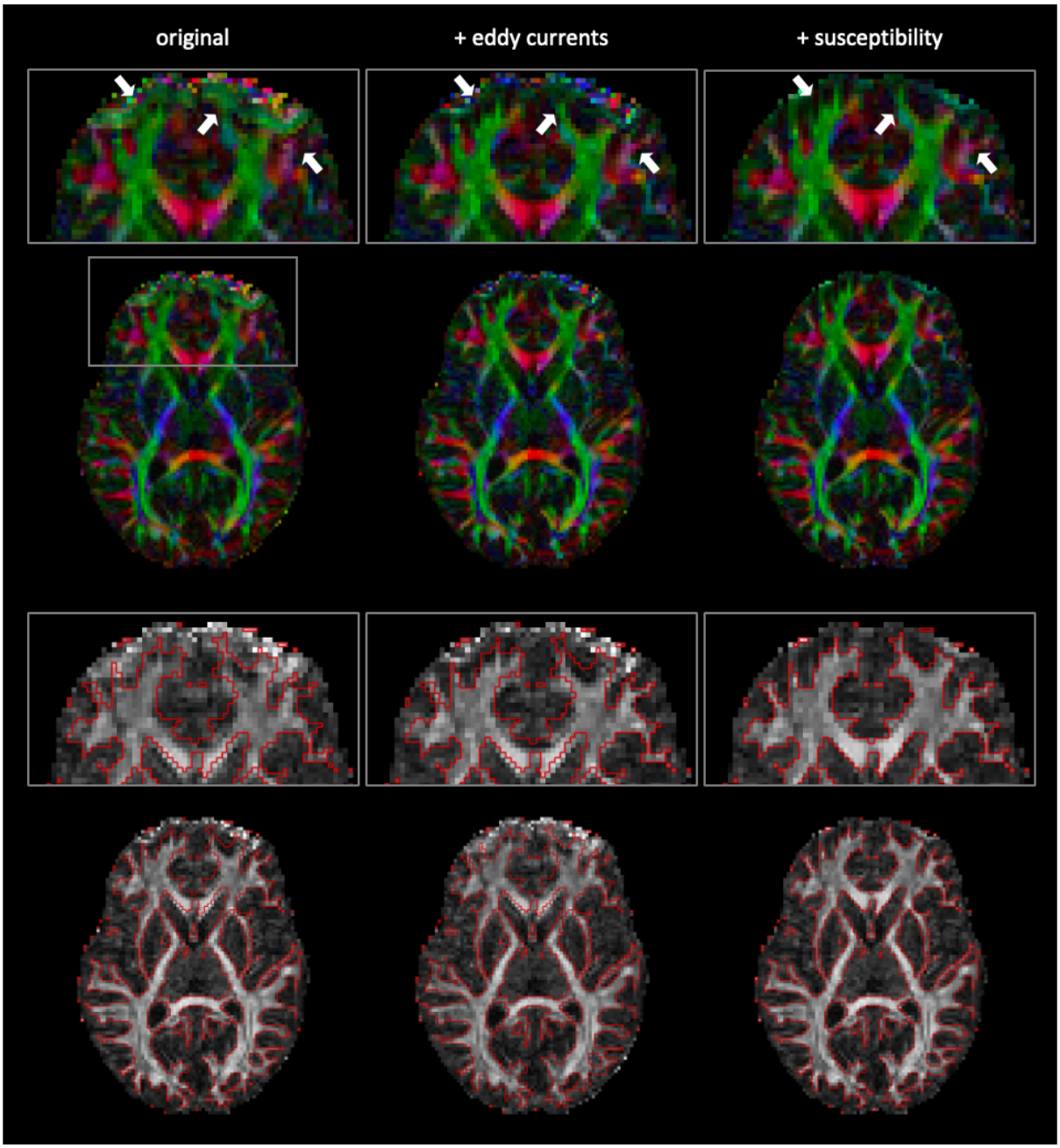

FIGURE 7. Eddy current and susceptibility distortions in DWI. The original data (left) suffers from both types of distortions leading to a gross mismatch between the image and the subject's real anatomy, and leads to false representations of local directional and microstructural information. Correcting for eddy current distortions (middle) improves the anatomical accuracy of the data and the robustness of the diffusion-derived metrics, but areas with high susceptibility distortions remain misaligned with the real anatomy (red contours). Only by including all corrections (right) does one obtain a dataset with high anatomical fidelity.

Thermal noise

Noise is an inherent challenge in all signal measuring systems, ranging from cameras to MRI scanners. Thermal noise, for instance, is the signal detected when an MRI scanner operates without scanning any object — instead of capturing a completely black image with zeros in every voxel, the resulting image will display a somewhat random array of non-zero values. This occurs because various scanner components inadvertently add some signal to the image, even in the absence of a person in the scanner. DWI is particularly susceptible to this problem due to its dependence on signal attenuation for acquiring information. The issue becomes more pronounced with the use of higher b-values, a characteristic aspect of HARDI data. Separating noise from the actual signal in the acquired image makes image de-noising a complex task. However, several contemporary methods have been developed with impressive results, significantly enhancing both the overall image quality and the effectiveness of tractography (Fadnavis et al., 2020; Veraart et al., 2016a).

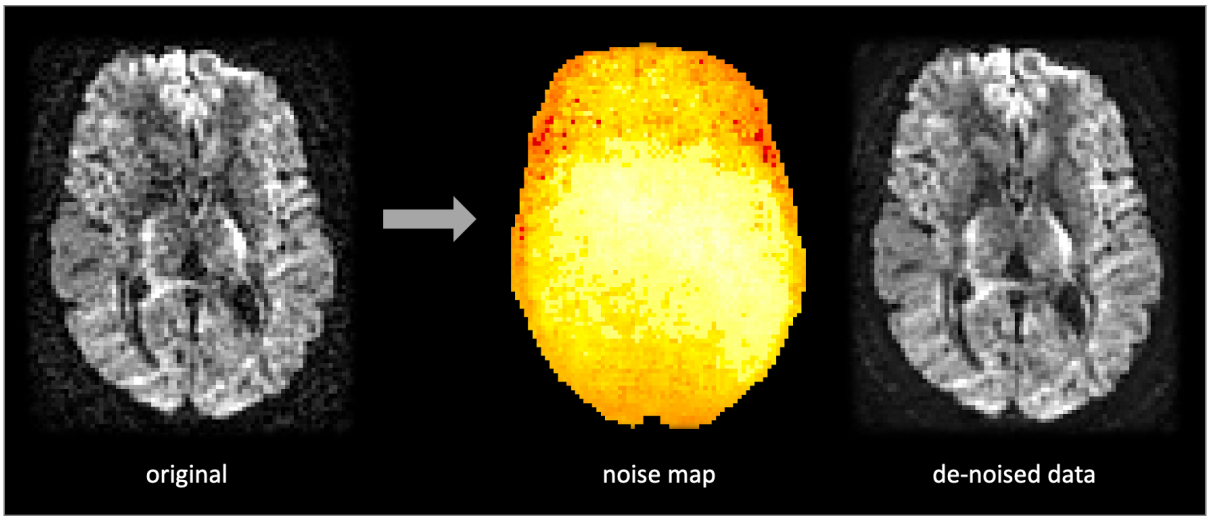

FIGURE 9. Denoising diffusion data. The acquired signal can be noisy, and several approaches have been proposed to compensate for this problem during image pre-processing. These estimate the noise distribution from the data and yield a cleaner output that improves modelling.

Gibbs ringing artefacts

A common image artefact observed in DWI at the interface between two regions with very different signal intensities is Gibbs ringing (Perrone et al., 2015; Veraart et al., 2016b). This artefact causes incorrect signal values around these border regions, e.g. it can

appear as 'ripples' of rapidly fluctuating signal intensity, where the signal should otherwise be stable or smoothly varying.

A robust pre-processing pipeline for neurosurgery

Incorporating adjustments for all the previously mentioned artefacts is a crucial component of contemporary DWI pre-processing workflows. However, while some of these corrections are deemed essential, others are considered beneficial but not mandatory.

At a minimum, adjustments for inter-volume motion and eddy current distortions are imperative — data that has not undergone these corrections is generally deemed unsuitable for any form of analysis. In the case of intra-volume motion, if the employed tools do not incorporate signal dropout regeneration, this aspect needs to be addressed during model fitting. Similarly, for slice-wise motion correction: if it is impossible to correct it, then any volumes exhibiting obvious intra-volume motion artefacts that the pre-processing software cannot manage should be excluded.

Other steps can be added to the pipeline as needed depending on data quality. For instance, if the acquired images have a high SNR and a relatively small amount of Gibbs ringing, one could choose to omit these steps if faced with limited time or computational resources. However, it is recommended that a full correction is applied for all the possible sources of artefacts mentioned earlier (Ades-Aron et al., 2018).

Importantly, the pre-processing pipeline must follow a specific order. For instance, if denoising were to be performed, it must be the first step in the pipeline applied directly to the raw images. Otherwise, other steps can alter the noise information contained in the images, especially if these steps include data interpolation (this is the case for motion and geometric corrections). Therefore, a full pre-processing pipeline would follow this scheme, in order: (1) denoising; (2) Gibbs ringing correction; (3) motion and eddy current correction; (4) susceptibility correction. Depending on the tools used, step 4 is sometimes incorporated into step 3 to avoid multiple interpolations of the images. However, this is not always possible (see section on susceptibility correction).

In essence, from the foundational corrections to desired improvements and the incorporation of advanced refinements, the journey to acquire and process advanced

tractography data involves a strategic orchestration of steps, each contributing to the fidelity and depth of insights derived from neuroimaging data.

Part 2: Clinical integration of advanced tractography

As of the date of this chapter (January 2024), the most prominent clinically certified or approved systems for white matter tractography mainly revolve around DTI. In clinical practice, there are some 'push button' solutions that only address a subset of these correction steps or offer advanced modelling tools, such as those offered by the Medtronic StealthStation™ Surgical Navigation System, or Imeka's Advanced Neuro Diagnostic Imaging. However, the more advanced tools for data pre-processing and modelling are, unfortunately, still confined to research use.

Tractography finds its primary applications in neurosurgery and epileptology, playing a pivotal role across three crucial stages: preoperative, intraoperative, and postoperative.

Neurosurgical preoperative visualisation

Several instances within the clinical workflow benefit from tractography results in neurosurgery. Preoperatively, the 3D visual depiction of a network in relation to a lesion is a crucial tool for strategic surgical planning that aims to preserve functions postoperatively as well as possible. Such a priori 3D images have been shown to aid in planning entry zones to the tumour and, importantly, safe resection margins, especially when used by less experienced clinicians (Ille et al., 2021a). Advanced tractography is hence a great candidate for detailed preoperative anatomical guidance. Nonetheless, high expertise in anatomy and tractography methods is needed to produce such tractograms. Moreover, the steps delineated earlier in this chapter are often deemed too time-consuming for the average clinical workflow, so the more time-efficient 'blackbox' solutions offered by built-in clinical software are often preferred. Future investigations will show if a more balanced consensus can be found.

In the preoperative phase, tractography's utility lies in meticulously assessing brain lesions. This assessment is then intricately compared with an in-depth evaluation of the patient's cognitive status, benchmarked against established norms. This comparative analysis is vital for the validation of tractography outcomes. A significant indicator of tractography's precision is when the imaged infiltration of white matter tracts corresponds with cognitive impairments, as predicted by the tracts' known functions (Forkel et al., 2022). Such congruence lends substantial credence to tractography's findings. These correlation studies have been conducted with DTI-based tractography, highlighting its utility in clinical neuroimaging.

Intraoperative fibre identification

Intraoperative direct electrical stimulation (DES) is the most direct way to interrogate the brain. However, caution has to be taken once the subcortical white matter is exposed: as already evident in preoperative tractograms, most areas are densely packed with multiple fibre bundles of interest. This makes it impossible to confirm that the exposed white matter during surgery presents solely and precisely the tract of interest. In the case of desired language preservation, for example, awake surgery cases often harbour lesions within or near the densely packed language network. It becomes a challenging task to disentangle tracts from each other without being able to verify them based on their respective cortical endpoints. This becomes particularly taxing for areas with tracts that have aligning trajectories, such as the arcuate fasciculus (AF) and the SLF along their dorsal trajectory, or the inferior longitudinal fasciculus (ILF) and inferior fronto-occipital fasciculus (IFOF) in the ventral stream (Weiler et al., 2021; Yagmurlu et al., 2017). An even greater risk of false identification lies in areas of tract crossroads, such as the temporo-parieto-occipital (TPO) junction where the AF, ILF, and IFOF pass through the same neighbourhood. Not only does this make identification and theoretical claims about the single tracts and their function ambitious, but it also renders this area a difficult and potentially unsafe entry zone for tumour removal (Tuncer et al., 2021).

Only a limited number of hospitals can conduct intraoperative tractography analysis, necessitating an intraoperative MRI (ioMRI) setup. This sophisticated arrangement permits the scanning of patients during surgery. However, implementing such a system

is costly, demands specialised expertise, and tends to extend the duration of surgical procedures. These factors contribute to its limited availability and use in clinical settings. Even though there is a possibility for immediate intraoperative tractography through ioMRI, preoperatively prepared network analyses are often favoured and can be uploaded to the intraoperative neuronavigation system. However, it is relevant to note that preoperative segmentation of tracts is performed on data acquired in a supine position with an intact skull. That setup can be dramatically different from the surgical one where patients are placed in any position necessary to facilitate access to the tumour, and where bone and tissue removal lead to tissue displacement (or brain shift). Once the craniotomy is completed and the resection commences and progresses, recurrent, reliable, and precise co-registration of imaging to the ever-changing neuroanatomy would be required. Swelling after opening and brain shift commonly cause distortion of anatomy (Gerard et al., 2017), hence calling for continuously applied correction throughout the various stages of the operation. This can be done through software-based distortion corrections and elastic fusion techniques, and/or by acquiring new intraoperative images (Zhang et al., 2022; Ille et al., 2021b). The time restriction often precludes a newly segmented tractogram based on the novel ioMR images, also due to often lower resolution of ioMRI (Nimsky et al., 2011; Maesawa et al., 2010). Hence, aligning the new ioMRI with the prepared tractogram and anatomy is recommended and shows good concordance with intraoperative testing of motor areas and function (Zhang et al., 2022).

Functional white matter mapping during surgery

For motor functions, the stimulation of white matter tracts can be done with the patient asleep by measuring MEPs elicited by stimulation on the patient's extremities, thereby localising motor areas and the CST (Bello et al., 2008; Zhu et al., 2012). For more complex functions, such as attention, facial recognition, and language, an awake and cooperative patient is required (De Witt Hamer, 2012; Ruis, 2018). Under local sedation for the invasive procedure on the scalp and skull, the patient is woken up to full consciousness and asked to perform specific behavioural and cognitive tasks [cross-reference other chapter]. Stimulation of (sub-)cortical areas and/or white matter tracts using DES then disrupts local action potentials in those areas (Berger & Ojemann, 1992; Duffau et al., 2015; Vanderweyen et al., 2020). If a stimulated area or tract contributes to performing the

assessed task, the patient's performance will be affected. The preoperatively segmented tractogram's validation is, then, based on the assumed function of the exposed white matter tract and its ability to disrupt the respective function when stimulated. For example, after preoperative tracking of the IFOF with advanced tractography and successful registration of the 3D reconstruction to the patient's intraoperative neuroanatomy, it can be located during the resection of affected white matter. If stimulation of the IFOF disrupts the function being tested, then the IFOF's involvement in that function (whether directly or indirectly) is confirmed (Duffau et al., 2005). Studies report a high concordance between tractography and DES, where 82-97% of DES sites corresponded to the expected locations derived from DTI-based preoperative tractography (Bello et al., 2007, 2008; Berman et al., 2007; Leclerq et al., 2010). Future investigations employing advanced tractography methods coupled with DES stimulation may improve this concordance by resolving some of the remaining discrepancies.

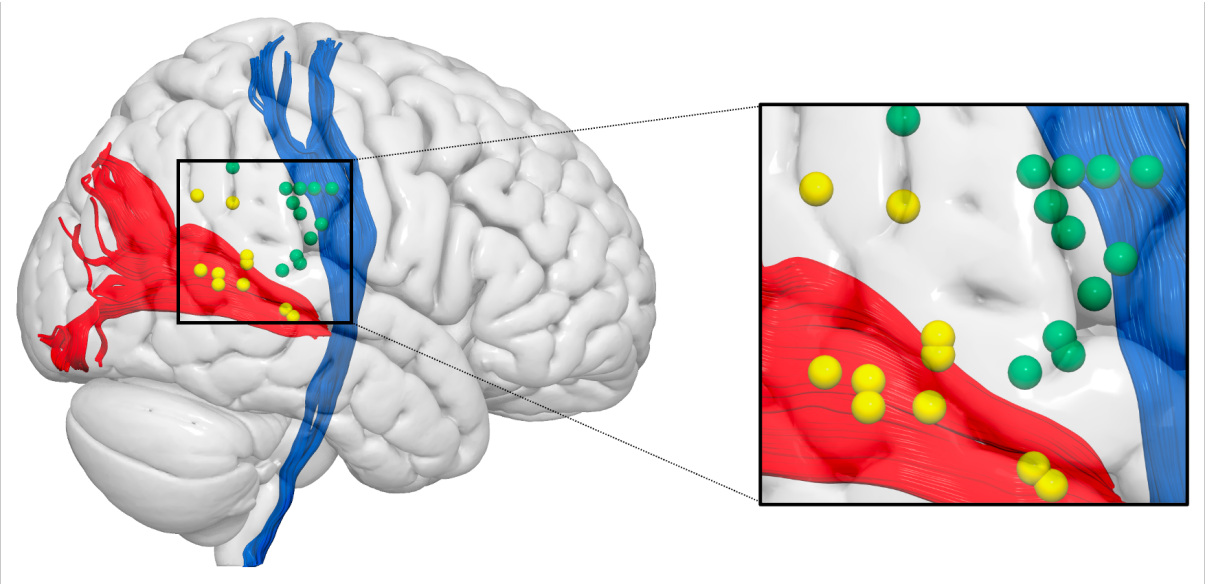

FIGURE 10. Tractography and surgical mapping. Illustration depicting independent reconstruction tractography and mapping points, i.e., nMTS was not used as a seed [cross-ref to our other chapter in this book], showing positive subcortical responses associated with the optic radiations and corticospinal tract at the group-level. The single-subject representation of the corticospinal tract is represented in blue, while the optic radiations are depicted in red. Yellow spheres denote positive subcortical responses for optic radiations induced by high-frequency bipolar stimulation, and green spheres signify positive subcortical responses for the corticospinal tract elicited through high-frequency monopolar stimulation at the group-level. Data based on Rajashekar et a. (2022).

Postoperative fibre identification

In the postoperative stage, tractography is invaluable for analysing neuroanatomical alterations, such as changes in the lesion cavity, by contrasting these with preoperative imaging and tractography findings. This comparison is essential to discern the relationship between anatomical shifts and variations in patient behaviour. Behavioural evaluations are typically undertaken in the short term, within the initial three months following surgery, and over the longer term, at follow-up assessments at six, nine, and 12 months. These post-surgical evaluations, crucial for gauging the success and impact of neurosurgical procedures, have primarily been conducted utilising DTI-based tractography, emphasising its importance in ongoing patient monitoring and understanding surgical outcomes over time (Carraba et al., 2022; Voets et al., 2021). As we highlighted earlier, though, such longitudinal monitoring would highly benefit from more robust and advanced methods that reveal information about each tract of interest based on fibre-specific metrics.

Integration of tractography and navigated TMS (nTMS)

Tractography results constantly face the challenge of balance between the over- and underrepresentation of fibres. Coupled with a functional mapping tool, subsets of tracts can be selected. This subset could be defined by functional involvement as delineated through fMRI activation (for a recent review, see Pasquini et al., 2023). A second option is stimulation mapping through DES or its preoperative counterpart, navigated transcranial magnetic stimulation (nTMS). nTMS pulses can be applied to the skull and reach the cortex (depth estimate: 20-30mm) to interrogate an area's functionality [cross-ref to our other chapter]. However, while nTMS is the closest match to DES and is non-invasive in nature, it does not reach the depth of white matter tracts (same applies to fMRI mapping). Nonetheless, cortical functional areas identified with nTMS can be used as regions of interest for tractography (see Chapter "Tractography for Language'; Negwer et al., 2017; Sollmann et al., 2016). In line with high-resolution tractography results, nTMS-based cortical areas can be uploaded to intraoperative neuronavigation and co-registered to structural anatomical images of a patient to aid the resection workflow (Sollmann et al.,

2018). Alternatively, as is shown in Figure 10, the tractography and functional mapping can be done independently to reconstruct the full structural and functional network and then co-visulised to identify the relevant overlap. This approach results in a complete network map for the structural and functional networks and is therefore preferable over the partial reconstruction of functional seed-based tractography. As a future goal, projects may combine nTMS maps of cortical functionality with high-resolution advanced tractography to highlight tracts and identify the full structural and functional network implicated by the presence and/or resection of a brain tumour.

Concluding remarks

This chapter has emphasised the transformative role of DWI and tractography in neurosurgery, offering unique insights into the brain's white matter tracts. While current clinical practice predominantly utilises DTI for its simplicity, there is significant potential for more advanced tractography methods, such as those based on the HARDI family of methods, particularly spherical deconvolution, to be integrated into standard clinical protocols.

The importance of tractography in preoperative, intraoperative, and postoperative stages highlights its impact on enhancing patient outcomes. Nevertheless, challenges such as the necessity for specialised sequences, preprocessing pipelines, and the analysis time remain barriers to its widespread adoption.

The future of tractography in clinical practice is promising, particularly with the potential integration with functional mapping tools like nTMS. This could lead to more precise and personalised neurosurgical interventions. As we continue to advance our understanding and technology, tractography stands on the brink of significantly revolutionising neurosurgical practice and improve longterm behavioural-cognitive coutcomes. This chapter underscores the importance of these neuroimaging techniques' ongoing development and clinical integration.

Acknowledgements

We thank the members of the CNSlab for discussions and feedback.

Funding

This project received funding from the Donders Theme Leadership Award (SJF, LANGUAGE & COMMUNICATION) and the Donders Mohrmann Fellowship No. 2401515 (SJF, NEUROVARIABILITY).

References

Ades-Aron, B., Veraart, J., Kochunov, P., McGuire, S., Sherman, P., Kellner, E., Novikov, D. S., & Fieremans, E. (2018). Evaluation of the accuracy and precision of the diffusion parameter EStImation with Gibbs and NoisE removal pipeline. NeuroImage, 183, 532–543. https://doi.org/10.1016/J.NEUROIMAGE.2018.07.066

Andersson, J. L. R., & Sotiropoulos, S. N. (2016). An integrated approach to correction for off-resonance effects and subject movement in diffusion MR imaging. NeuroImage, 125, 1063–1078. https://doi.org/10.1016/j.neuroimage.2015.10.019

Andersson, J. L. R., Graham, M. S., Drobnjak, I., Zhang, H., Filippini, N., & Bastiani, M. (2017). Towards a comprehensive framework for movement and distortion correction of diffusion MR images: Within volume movement. NeuroImage, 152(March), 450–466. https://doi.org/10.1016/j.neuroimage.2017.02.085

Andersson, J. L. R., Graham, M. S., Zsoldos, E., & Sotiropoulos, S. N. (2016). Incorporating outlier detection and replacement into a non-parametric framework for movement and distortion correction of diffusion MR images. NeuroImage, 141, 556–572. https://doi.org/10.1016/j.neuroimage.2016.06.058

Andersson, J. L. R., Skare, S., & Ashburner, J. (2003). How to correct susceptibility distortions in spin-echo echo-planar images: Application to diffusion tensor imaging. NeuroImage, 20(2), 870–888. https://doi.org/10.1016/S1053-8119(03)00336-7

Basser, P. J., Pajevic, S., Pierpaoli, C., Duda, J., & Aldroubi, A. (2000). In vivo fiber tractography using DT-MRI data. Magnetic Resonance in Medicine, 44, 625–632. https://doi.org/10.1002/1522-2594(200010)44:4

Behrens, T. E. J., Berg, H. J., Jbabdi, S., Rushworth, M. F. S., & Woolrich, M. W. (2007). Probabilistic diffusion tractography with multiple fibre orientations: What can we gain? NeuroImage, 34(1), 144–155. https://doi.org/10.1016/j.neuroimage.2006.09.018

Bello, Lorenzo, Marcello Gallucci, Marica Fava, Giorgio Carrabba, Carlo Giussani, Francesco Acerbi, Pietro Baratta et al. "Intraoperative subcortical languagetract mapping guides surgical removalof gliomas involving speech areas." Neurosurgery 60, no. 1 (2007): 67-82.

Bello L, Gambini A, Castellano A, et al. Motor and language DTI fiber tracking combined with intraoperative subcortical mapping for surgical removal of gliomas. Neuroimage. 2008; 39(1): 369-382.

Berger MS, Ojemann GA (1992) Intraoperative brain mapping techniques in neuro-oncology. Stereotact Funct Neurosurg 58(1–4):153–161

Berman, J. I., Berger, M. S., Chung, S., Nagarajan, S. S., & Henry, R. G. (2007). Accuracy of diffusion tensor magnetic resonance imaging tractography assessed using intraoperative subcortical stimulation mapping and magnetic source imaging. Journal of neurosurgery, 107(3), 488-494.

Carrabba, G., Fiore, G., Di Cristofori, A., Bana, C., Borellini, L., Zarino, B., Conte, G., Triulzi, F., Rocca, A., Giussani, C. and Caroli, M., 2022. Diffusion tensor imaging, intra-operative neurophysiological monitoring and small craniotomy: results in a consecutive series of 103 gliomas. Frontiers in Oncology, 12, p.897147.

Chang, L. C., Jones, D. K., & Pierpaoli, C. (2005). RESTORE: Robust estimation of tensors by outlier rejection. Magnetic Resonance in Medicine, 53(5), 1088–1095. https://doi.org/10.1002/mrm.20426

Dell'Acqua, F., & Catani, M. (2012). Structural human brain networks: Hot topics in diffusion tractography. Current Opinion in Neurology, 25(4), 375–383. https://doi.org/10.1097/WCO.0b013e328355d544

Dell'Acqua, F., & Tournier, J. -Donal. (2019). Modelling white matter with spherical deconvolution: How and why? NMR in Biomedicine, 32(4), e3945. https://doi.org/10.1002/nbm.3945

Dell'Acqua, F., Scifo, P., Rizzo, G., Catani, M., Simmons, A., Scotti, G., & Fazio, F. (2010). A modified damped Richardson-Lucy algorithm to reduce isotropic background effects in spherical deconvolution. NeuroImage, 49(2), 1446–1458. https://doi.org/10.1016/j.neuroimage.2009.09.033

Dell'Acqua, F., Simmons, A., Williams, S. C. R., & Catani, M. (2013). Can spherical deconvolution provide more information than fiber orientations? Hindrance modulated orientational anisotropy, a true-tract specific index to characterize white matter diffusion. Human Brain Mapping, 34(10), 2464–2483. https://doi.org/10.1002/hbm.22080

Descoteaux, M., Deriche, R., Knösche, T. R., & Anwander, A. (2009). Deterministic and probabilistic tractography based on complex fibre orientation distributions. IEEE Transactions on Medical Imaging, 28(2), 269–286. https://doi.org/10.1109/TMI.2008.2004424

De Witt Hamer PC, Robles SG, Zwinderman AH, Duffau H, Berger MS (2012) Impact of intraoperative stimulation brain mapping on glioma surgery outcome: a meta-analysis. J Clin Oncol 30(20):2559–2565

Doricchi, F. (2022). The functions of the temporal–parietal junction. Handbook of Clinical Neurology, 187, 161-177.

Duffau, H., Gatignol, P., Mandonnet, E., Peruzzi, P., Tzourio-Mazoyer, N., & Capelle, L. (2005). New insights into the anatomo-functional connectivity of the semantic system: a study using cortico-subcortical electrostimulations. Brain, 128(4), 797-810.

Duffau, H. (2015). Stimulation mapping of white matter tracts to study brain functional connectivity. Nature Reviews Neurology, 11(5), 255-265.

Fadnavis, S., Batson, J., & Garyfallidis, E. (2020). Patch2Self: Denoising diffusion MRI with self-supervised learning. Advances in Neural Information Processing Systems, 2020-Decem(NeurIPS).

Forkel, S., & Catani, M. (2017). Structural neuroimaging. In A. M. B. de Groot & P. Hagoort (Eds.), Research methods in psycholinguistics and the neurobiology of language: a practical guide (p. 371). Wiley & Sons. https://www.wiley.com/en-us/Research+Methods+in+Psycholinguistics+and+the+Neurobiology+of+Language%3A+A+Practical+Guide-p-9781119109846

Forkel, S. J., Labache, L., Nachev, P., Thiebaut de Schotten, M., & Hesling, I. (2022). Stroke disconnectome decodes reading networks. Brain Structure and Function, 227, 2897–2908. https://doi.org/10.1007/S00429-022-02575-X/FIGURES/3

Forkel, S. J., Thiebaut De Schotten, M., Dell'Acqua, F., Kalra, L., Murphy, D. G. M., Williams, S. C. R., & Catani, M. (2014). Anatomical predictors of aphasia recovery: A tractography study of bilateral perisylvian language networks. Brain, 137(7), 2027–2039. https://doi.org/10.1093/brain/awu113

Gerard IJ, Kersten-Oertel M, Petrecca K, Sirhan D, Hall JA, Collins DL. Brain shift in neuronavigation of brain tumors: a review. Med Image Anal. 2017; 35: 403-420.

Ille, S., Ohlerth, A.K., Colle, D., Colle, H., Dragoy, O., Goodden, J., Robe, P., Rofes, A., Mandonnet, E., Robert, E. and Satoer, D., 2021b. Augmented reality for the virtual dissection of white matter pathways. Acta neurochirurgica, 163, pp.895-903.

Ille, S., Schwendner, M., Zhang, W., Schroeder, A., Meyer, B., & Krieg, S. M. (2021a). Tractography for subcortical resection of gliomas is highly accurate for motor and language function: ioMRI-based elastic fusion disproves the severity of brain shift. Cancers, 13(8), 1787.

Jones, D. K. (Ed.). (2010). Diffusion MRI: Theory, Methods, and Applications. Oxford Academic. https://doi.org/10.1093/MED/9780195369779.001.0001

Kellner, E., Dhital, B., Kiselev, V. G., & Reisert, M. (2016). Gibbs-ringing artifact removal based on local subvoxel-shifts. Magnetic Resonance in Medicine, 76(5), 1574–1581. https://doi.org/10.1002/mrm.26054

Le Bihan, D., & Johansen-Berg, H. (2012). Diffusion MRI at 25: Exploring brain tissue structure and function. NeuroImage, 61(2), 324–341. https://doi.org/10.1016/J.NEUROIMAGE.2011.11.006

Le Bihan, D. (2013). Apparent diffusion coefficient and beyond : What diffusion MR imaging can tell us about tissue structure. Radiology, 268(2), 318–322. https://doi.org/10.1148/radiol.13130420

Leclercq, D., Duffau, H., Delmaire, C., Capelle, L., Gatignol, P., Ducros, M., Chiras, J. and Lehéricy, S., 2010. Comparison of diffusion tensor imaging tractography of language tracts and intraoperative subcortical stimulations. Journal of neurosurgery, 112(3), pp.503-511.

Maesawa S, Fujii M, Nakahara N, Watanabe T, Wakabayashi T, Yoshida J. Intraoperative tractography and motor evoked potential (MEP) monitoring in surgery for gliomas around the corticospinal tract. World Neurosurg. 2010; 74(1): 153-161.

Negwer, C., Ille, S., Hauck, T., Sollmann, N., Maurer, S., Kirschke, J.S., Ringel, F., Meyer, B. and Krieg, S.M., 2017. Visualization of subcortical language pathways by diffusion tensor imaging fiber tracking based on rTMS language mapping. Brain imaging and behavior, 11, pp.899-914.

Nimsky C. Intraoperative acquisition of fMRI and DTI. Neurosurg Clin N Am. 2011; 22(2): 269-77, ix.

Pasquini, L., Peck, K. K., Jenabi, M., & Holodny, A. (2023). Functional MRI in Neuro-Oncology: State of the Art and Future Directions. Radiology, 308(3), e222028.

Rajashekar, D., Lavrador, J. P., Ghimire, P., Keeble, H., Harris, L., Pereira, N., Patel, S., Beyh, A., Gullan, R., Ashkan, K., Bhangoo, R., & Vergani, F. (2022). Simultaneous motor and visual intraoperative neuromonitoring in asleep parietal lobe surgery: dual strip technique. Journal of Personalized Medicine, 12(9), 1478. https://doi.org/10.3390/JPM12091478

Rosenstock, T., Grittner, U., Acker, G., Schwarzer, V., Kulchytska, N., Vajkoczy, P., & Picht, T. (2017). Risk stratification in motor area–related glioma surgery based on navigated transcranial magnetic stimulation data. Journal of neurosurgery, 126(4), 1227-1237.

Ruis, C. (2018). Monitoring cognition during awake brain surgery in adults: a systematic review. Journal of clinical and experimental neuropsychology, 40(10), 1081-1104.

Schilling, K. G., Blaber, J., Hansen, C., Cai, L., Rogers, B., Anderson, A. W., Smith, S., Kanakaraj, P., Rex, T., Resnick, S. M., Shafer, A. T., Cutting, L. E., Woodward, N., Zald, D., & Landman, B. A. (2020). Distortion correction of diffusion weighted MRI without reverse phase-encoding scans or field-maps. PLOS ONE, 15(7), e0236418. https://doi.org/10.1371/JOURNAL.PONE.0236418

Schilling, K. G., Nath, V., Hansen, C., Parvathaneni, P., Blaber, J., Gao, Y., Neher, P., Aydogan, D. B., Shi, Y., Ocampo-Pineda, M., Schiavi, S., Daducci, A., Girard, G., Barakovic, M., Rafael-Patino, J., Romascano, D., Rensonnet, G., Pizzolato, M., Bates, A., … Landman, B. A. (2019). Limits to anatomical accuracy of diffusion

tractography using modern approaches. NeuroImage, 185, 1–11. https://doi.org/10.1016/J.NEUROIMAGE.2018.10.029

Sollmann, N., Kelm, A., Ille, S., Schröder, A., Zimmer, C., Ringel, F., Meyer, B. and Krieg, S.M., 2018. Setup presentation and clinical outcome analysis of treating highly language-eloquent gliomas via preoperative navigated transcranial magnetic stimulation and tractography. Neurosurgical focus, 44(6), p.E2.

Sollmann, N., Negwer, C., Ille, S., Maurer, S., Hauck, T., Kirschke, J.S., Ringel, F., Meyer, B. and Krieg, S.M., 2016. Feasibility of nTMS-based DTI fiber tracking of language pathways in neurosurgical patients using a fractional anisotropy threshold. Journal of neuroscience methods, 267, pp.45-54

Stejskal, E. O., & Tanner, J. E. (1965). Spin diffusion measurements: Spin echoes in the presence of a time-dependent field gradient. The Journal of Chemical Physics, 42(1), 288–292. https://doi.org/10.1063/1.1695690

Thiebaut de Schotten, M., Dell'Acqua, F., Forkel, S. J., Simmons, A., Vergani, F., Murphy, D. G. M., & Catani, M. (2011). A lateralized brain network for visuospatial attention. Nature Neuroscience, 14(10), 1245–1246. https://doi.org/10.1038/nn.2905

Tournier, J. D., Mori, S., & Leemans, A. (2011). Diffusion tensor imaging and beyond. Magnetic Resonance in Medicine, 65(6), 1532–1556. https://doi.org/10.1002/mrm.22924

Tuch, D. S. (2004). Q-ball imaging. Magnetic Resonance in Medicine, 52(6), 1358–1372. https://doi.org/10.1002/MRM.20279

Tuncer, M. S., Salvati, L. F., Grittner, U., Hardt, J., Schilling, R., Bährend, I., Silva, L. L., Fekonja, L. S., Faust, K., Vajkoczy, P., Rosenstock, T., & Picht, T. (2021). Towards a tractography-based risk stratification model for language area associated gliomas. NeuroImage: Clinical, 29, 102541. https://doi.org/10.1016/J.NICL.2020.102541

Vanderweyen, D. C., Theaud, G., Sidhu, J., Rheault, F., Sarubbo, S., Descoteaux, M., & Fortin, D. (2020). The role of diffusion tractography in refining glial tumor resection. Brain Structure and Function, 225, 1413-1436.

Veraart, J., Fieremans, E., & Novikov, D. S. (2016a). Diffusion MRI noise mapping using random matrix theory. Magnetic Resonance in Medicine, 76(5), 1582–1593. https://doi.org/10.1002/mrm.26059

Veraart, J., Fieremans, E., & Novikov, D. S. (2019). On the scaling behavior of water diffusion in human brain white matter. NeuroImage, 185, 379–387. https://doi.org/10.1016/J.NEUROIMAGE.2018.09.075

Veraart, J., Fieremans, E., Jelescu, I. O., Knoll, F., & Novikov, D. S. (2016b). Gibbs ringing in diffusion MRI. Magnetic Resonance in Medicine, 76(1), 301–314. https://doi.org/10.1002/MRM.25866

Voets, N. L., Pretorius, P., Birch, M. D., Apostolopoulos, V., Stacey, R., & Plaha, P. (2021). Diffusion tractography for awake craniotomy: accuracy and factors affecting specificity. *Journal of Neuro-oncology*, *153*(3), 547-557.

Wedeen, V. J., Hagmann, P., Tseng, W. Y. I., Reese, T. G., & Weisskoff, R. M. (2005). Mapping complex tissue architecture with diffusion spectrum magnetic resonance imaging. Magnetic Resonance in Medicine, 54(6), 1377–1386. https://doi.org/10.1002/MRM.20642

Weiller, C., Reisert, M., Peto, I., Hennig, J., Makris, N., Petrides, M., Rijntjes, M. and Egger, K., 2021. The ventral pathway of the human brain: A continuous association tract system. NeuroImage, 234, p.117977.

Yendiki, A., Aggarwal, M., Axer, M., Howard, A. F. D., van Walsum, A. M. van C., & Haber, S. N. (2022). Post mortem mapping of connectional anatomy for the validation of diffusion MRI. NeuroImage, 256, 119146. https://doi.org/10.1016/J.NEUROIMAGE.2022.119146

Zhang, W., Ille, S., Schwendner, M., Wiestler, B., Meyer, B. and Krieg, S.M., 2022. Tracking motor and language eloquent white matter pathways with intraoperative fiber tracking versus preoperative tractography adjusted by intraoperative MRI–based elastic fusion. Journal of Neurosurgery, 137(4), pp.1114-1123.

Zhu, F.P., Wu, J.S., Song, Y.Y., Yao, C.J., Zhuang, D.X., Xu, G., Tang, W.J., Qin, Z.Y., Mao, Y. and Zhou, L.F., 2012. Clinical application of motor pathway mapping using diffusion tensor imaging tractography and intraoperative direct subcortical stimulation in cerebral glioma surgery: a prospective cohort study. *Neurosurgery*, *71*(6), pp.1170-1184.

Online tutorials

Tutorial on Tractography data visualisation (https://youtu.be/L4KPpm2e4ck)

Tutorial for the SLF dissections (https://youtu.be/CojNe42RUjE).

Tutorial for the arcuate fasciculus (https://youtu.be/ypUSTD-5p1Q).

Lecture on Tractography methods (https://youtu.be/DpCb7uVivAk)

Lecture on Methods to study white matter (https://youtu.be/oX2Pgti8olQ)

Software and data used in this chapter

http://trackvis.org/

https://www.nitrc.org/projects/surfice/

https://www.humanconnectome.org/

http://www.bcblab.com/BCB/Opendata.html

https://www.stephanieforkel.com/opendata

https://www.exploredti.com/

https://www.mr-startrack.com/

https://fsl.fmrib.ox.ac.uk/fsl/fslwiki

https://www.mathworks.com/products/matlab.html

Figure permission log

Figure #	Title	Permission
1	Patterns of water diffusion	Author's original
2	Diffusion-weighted imaging	Author's original
3	Multifibre anatomy and their construction using DTI and SD	Author's original
4	Single fibre vs. multi-fibre tractography	Panel A: adopted from Dell'Acqua and Tournier (2019) with permission (CC-BY) Panels B,C: Author's original based on Dell'Acqua & Catani (2012)
5	Technical considerations involved in tractography reconstructions for brain tumours	Modified from OUR CHAPTER, with permission from the authors (we were the original creators of this figure)
6	Motion correction of diffusion images	Adapted from Andersson et al. (2017), with permission (CC-BY)
7	Eddy current and susceptibility distortions in DWI	Author's original
8	Denoising diffusion data	Author's original
9	Integration of TMS and tractography	Author's original
10	Tractography and surgical mapping	Author's original based on data from Rajashekar et al. (2022)